Comparison of Charge Estimators for Piezoelectric Actuators

Morteza Mohammadzaheri
Department of Engineering
Birmingham City Univerisity
Birmingham, UK
ORCID ID: 0000-0002-8187-6375

Sami AlSulti
Ministry of Housing and Urban Planning,
Muscat, Oman
ORCID ID: 0000-0002-2322-6382

Mojtaba Ghodsi
School of Energy & Electronic Engineering
University of Portsmouth
Portsmouth, UK
ORCID ID: 0000-0002-8762-9498

Payam Soltani
Department of Engineering
Birmingham City Univerisity
Birmingham, UK
ORCID ID: 0000-0002-8186-2678

***Abstract*—This article deals with charge estimators for piezoelectric actuators. Two most recent/effective types of these estimators employ either a sensing capacitor (type I in this paper) or a sensing resistor (type II); the latter (and the newer) one is widely called digital charge estimator. There are experimental results in the literature indicating that, with the same waste of voltage, significantly higher amount of charge can be estimated with a type II estimator compared to a type I one; thus, the superiority of type II estimators has been professed. In order to re-assess this conclusion, this paper even-handedly compares type I and II estimators through analytical modelling and experimentation. The results show that types II estimators only have an insubstantial advantage in estimating higher amount of charge, if both type I and II estimators are designed pertinently. On the other hand, the resistance of type II estimators needs to tuned to deal with different excitation frequencies. This research concludes that capacitor-based charge estimators of piezoelectric actuators, with proper design and implementation, can be still the right solution for many problems despite the claims in the literature in the last decade.**

***Keywords*—piezoelectric, charge, actuator, capacitor, nanopositioning**

I. Introduction

In piezoelectric materials, electrical voltage generates deformation. This phenomenon is known as inverse piezoelectricity [1]. Piezoelectric devices, purposely fabricated to utilise inverse piezoelectricity, are known as piezoelectric actuators [2]. Piezoelectric are the foremost actuators in micro/ nanopositioning [3, 4].

Micro/nanopositioning aims at precise motion control at micro/nanometre scale. Fine machining [5], manipulation of biological cells [6, 7] , scanning probe microscopy [8] and precise robotic surgery [9] are some applications of micro/ nanopositioning with piezoelectric actuators or piezo-actuated micro/nanopositioning .

The key task in piezo-actuated micro/nanopositioning is precise control of the actuator position. Position of (an unfixed point/surface of) a piezoelectric actuator is its displacement from its relaxed state, when the actuator has not been subject to any electrical or mechanical excitation for a considerably long period of time (e.g. some minutes) [10]. Experiments have demonstrated that the position of a piezoelectric actuator is proportional to its electric charge for an extensive operating area [11, 12]. Therefore, a charge estimator can replace a costly and troublesome accurate position/displacement sensor; this motivates research on charge estimation of piezoelectric actuators [13, 14].

II. Problem Statement

Figures 1 and 2 depict the most promising types of charge estimator, mentioned as types I and II in this paper. Other (i.e. obsolete) types of charge estimators have been detailed in [15].

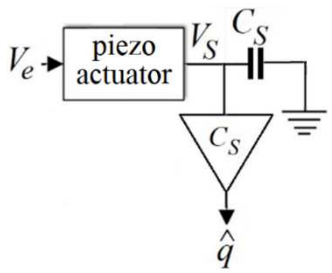

Fig. 1. Schematic of a charge estimator with a sensing capacitor and without any drift removal compoenent

Figure 1 is inspired by the pioneer work of [16], published in 1981. V_e is the excitation voltage, the voltage exerted to the actuator, and V_S is the sensing voltage, the voltage across the sensing element, i.e. the capacitor of C_S in Fig.1. As V_S is not applied on the actuator, it is also known as the voltage drop.

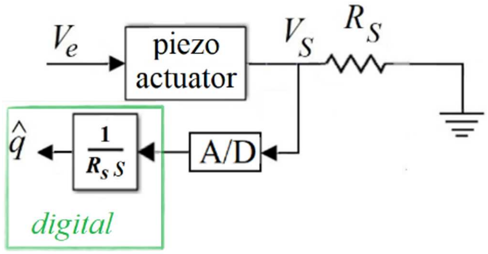

Fig. 2. A type II charge estimator with a sensing resistor

Equation (1) evidently presents V_S in Laplace domain:

$$V_S = \frac{I_S}{C_S s}. \quad (1)$$

where I_S is the current passing the sensing capacitor. The voltage amplifier (the triangle) is not grounded; thus, only a tiny current passes through it. Therefore, I_S is nearly equal to the current passing the piezoelectric actuator, I_P:

$$I_S \approx I_P = qs \tag{2}$$

where q is the charge of the piezoelectric actuator, and s is the Laplace variable. Combination of (1) and (2) shows that V_S, amplified by a voltage amplifier with a gain of C_S, can estimate the charge:

$$V_S \approx \frac{qs}{C_S s} = \frac{q}{C_S} \Rightarrow \hat{q} \approx C_S V_S \quad . \tag{3}$$

As to (3), the main role of the sensing capacitor in type I estimators is to add an integrator to make the sensing voltage proportional to the actuator's charge (rather than current). Such an integration; however, may happen within a digital processor with no need to a capacitor, as proposed in 2010 [17]. Figure 2 depicts a type II charge estimator with a sensing resistor, where A/D stands for analogue to digital converter. The current going towards A/D is tiny; hence, the current passing through the sensing resistor nearly equals I_P, the current passing the piezoelectric actuator. As a result, (4) presents the voltage across the sensing resistor:

$$V_S \simeq I_P R_S \, . \tag{4}$$

Equations (2 and 4) and $I_P = qs$ lead to (5):

$$V_S \approx I_P R_S = qsR_S \Rightarrow \hat{q} = \frac{V_S}{R_S s}. \tag{5}$$

Both type I and II charge estimators have two main drawbacks:

1. Existence of drift, a type of estimation error happening over time, detailed in [18].
2. The voltage across the sensing element, known as voltage drop, is not exerted on the actuator and is virtually wasted.

The first drawback can be tackled with use analogue or digital low pass filters along with a weighted filter or a data fusion algorithm as detailed in [11, 19] and is no longer discussed in this paper. No drift removal component is presented in this paper too, as they have negligible effect on the behaviour of the estimator apart from oppressing drift [11, 19].

The second drawback, voltage drop, is the remaining decisive matter in the choice of charge estimator type. Depending on the employed equipment, a certain value of voltage drop, V_S, is required for charge estimation without loss of accuracy, as detailed in [20]. The question is how much charge can be estimated with this inevitable voltage drop.

Experimental results reported in [21] demonstrate that a type II estimator witnesses significantly smaller voltage drop compared to a type I one, to estimate the same amount of charge. This conclusion can be reasonably rephrased as 'with same voltage drop, type II estimators can estimate much larger amount of charge than type I ones'. Therefore, it was concluded that type II estimators outperform type I ones in terms of voltage drop [15]. As a result, recent research in the area of charge estimation of piezoelectric actuators is mainly focused on type II (digital) charge estimators [18, 22].

This paper questions the superiority of type II charge estimators, demonstrated by experimental results of [21]. The key point is that the sensing element, either the capacitor in type I or the resistor in type II (digital) estimators, have been generally chosen intuitively in both type I (e.g. [23, 24]) and type II (e.g. [21, 25]) estimators. Therefore, no general conclusion can be drawn out of their comparison.

In this paper, the sensing element of type I and type II charge estimators are analytically selected so that, theoretically, both result in a voltage drop with the amplitude of 1 V for a number of sinusoidal excitation voltages. Then, they are analytically and experimentally compared in terms of their estimated charge and other performance factors. In this paper, term 'design' mainly refers to the choice of the sensing component.

In order to have an equitable comparison, this article proposes a new version of type I estimators, depicted in Fig.3, with a digital gain instead of the amplifier in Fig. 1. This proposed estimator, in terms of implementation, is well comparable to type II estimators depicted in Fig.2.

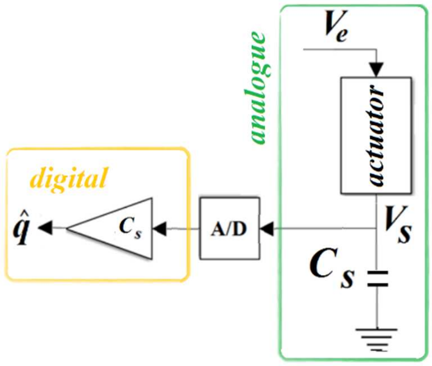

Fig. 3. Proposed implementation of a charge estimator with a sensing capacitor and a digital high pass filter and gain

III. Analytical Investigation

This section presents approximate analytical formulation of type I and II charge estimators, depicted in Figs. 3 and 2, respectively. The primary goal of this section is to suggest the sensing capacitance/resistance that leads to a certain voltage drop amplitudes for type I/II estimators. In this section, the tiny current going to A/D is neglected. In addition, the piezoelectric actuator is approximated by a capacitor, C_P [21].

A. Analytical formulation for type I charge estimators

With aforementioned assumptions, in Fig. 2, the piezoelectric actuator and the sensing capacitor are in series; therefore, (6 and 7) present their equivalent impedance, Z, and the current passing the actuator, I_P:

$$Z(s) = \frac{1}{C_P s} + \frac{1}{C_S s} = \frac{C_S + C_P}{C_S C_P s}. \tag{6}$$

$$I_P(s) = \frac{V_e(s)}{Z(s)} = V_e(s)\frac{C_S C_P s}{C_S + C_P} \, . \tag{7}$$

Using (7), (8) approximates the voltage drop, V_S:

$$V_S(s) = \underbrace{V_e(s)\frac{C_S C_P s}{C_S + C_P}}_{I_P} \times \frac{1}{C_S s} = V_e(s)\frac{C_P}{C_S + C_P} \, . \tag{8}$$

As to (8), V_S is proportional to the excitation voltage, V_e; therefore, a bias (time independent component) in V_e leads to a bias in V_S. In addition, with considering A_e and A_S as the amplitudes of sinusoidal V_e and V_S, respectively, (8) leads to (9):

$$A_S = A_e \frac{C_P}{C_S + C_P} \, . \tag{9}$$

B. Analytical formulation for type II charge estimators

For the system depicted in Fig.2, with assumptions presented at the begging of section III, (10-12) replace (6-8):

$$Z(s) = \frac{1}{C_P s} + R_S = \frac{1 + R_S C_P s}{C_P s}. \quad (10)$$

$$I_P(s) = V_e(s)\frac{C_P s}{1 + R_S C_P s}. \quad (11)$$

$$V_S(s) = \underbrace{V_e(s)\frac{C_P s}{1 + R_S C_P s}}_{I_P} \times R_S = V_e(s)\frac{R_S C_P s}{1 + R_S C_P s} \Rightarrow$$

$$\frac{V_S(s)}{V_e(s)} = \frac{R_S C_P s}{R_S C_P s + 1}. \quad (12)$$

For the approximate linear system presented by (12), a sinusoidal excitation voltage without a bias, $V_e = A_e \sin \omega t$, leads to a sensing voltage (also known as the voltage drop) of

$V_S = A_S (\sin \omega t + 0.5\pi - \tan^{-1} R_S C_P) \approx A_S \cos \omega t$. (13)

Considering the fact that C_P is a very small number, as mentioned in section IV, $\tan^{-1} R_S C_P \approx 0$.

Based on (12), the amplitudes of V_e and V_S, A_S and A_e, have the following relationship:

$$\frac{A_S}{A_e} = \left|\frac{R_S C_P j\omega}{R_S C_P j\omega + 1}\right| = \frac{R_S C_P \omega}{\sqrt{(R_S C_P \omega)^2 + 1}} \Rightarrow A_S\sqrt{(R_S C_P \omega)^2 + 1}$$

$$= A_e R_S C_P \omega \Rightarrow A_S^2\left((R_S C_P \omega)^2 + 1\right) = A_e^2 (R_S C_P \omega)^2$$

Hence, $A_S = \dfrac{A_e R_S C_P \omega}{\sqrt{1 + (R_S C_P \omega)^2}}$. (14)

For a sinusoidal excitation voltage with bias of B, i.e. $V_e = A_e \sin \omega t + B$, since (12) is linear, superposition may be used, and the sensing voltage, V_S, can be assumed as sum of two components influenced by $A_e \sin \omega t$ and B (bias or time independent excitations). The final value of the component of V_S, influenced by B, V_{SB}, is shown to be zero in (15):

$$\lim_{t\to\infty} V_{SB}(t) = \lim_{s\to 0} s V_{SB}(s) = \lim_{s\to 0} s \underbrace{\frac{R_S C_P s}{R_S C_P s + 1}}_{transfer\ function} \frac{B}{s} = 0. \quad (15)$$

That is, excitation bias has no enduring effect in type II charge estimator of piezoelectric actuators. This agrees with experimental results reported in [26].

C. Results of Approximate Analytical Investigation

Based on the formulation presented in subsections III.A and B, it is possible to find approximate sensing capacitance/resistance in type I/II estimators, leading to a certain voltage drop amplitude, A_S, for any given sinusoidal excitation voltage.

In type I estimators, as to (9), in order to achieve a voltage drop amplitude of A_S, for a given excitation voltage amplitude of A_e, the sensing capacitor should be chosen according to (16):

$$C_S = \frac{C_P (A_e - A_S)}{A_S}. \quad (16)$$

According to (8), a sinusoidal excitation voltage leads to a sinusoidal voltage drop. In this case, $q = C_S V_S = C_S A_S \sin \omega t$. Thus, $q_{range\text{-}I} = 2 C_S A_S$. (17)

where $q_{range\text{-}I}$ is the range of charge with type I estimator in the case of a voltage drop amplitude of A_S.

In type II estimators, with use of (3) and (13):

$$q(t) = \int_o^t I_P d\tau = \int_o^t \frac{V_S}{R_S} d\tau = \int_o^t \frac{A_S}{R_S}\cos \omega\tau d\tau = \frac{A_S}{R_S \omega}\sin \omega\tau \Big|_0^t$$

$$= \frac{A_S}{R_S \omega}\sin \omega t.$$

As a result, $q_{range\text{-}II} = \dfrac{2A_S}{R_S \omega}$. (18)

In addition, based on (14), (19) defines the sensing resistor leading to A_S:

$$R_S = \frac{1}{A_S C_P \omega \sqrt{A_e^2 - 1}}, \quad (19)$$

(18 and 19) lead to

$$q_{range\text{-}II} = 2 C_P A_S \sqrt{A_e^2 - 1} \approx 2 C_P A_S A_e. \quad (20)$$

Assuming $A_e \gg 1$ and with use of (9) and (20), (21) is derived to increase comparability of type I and II estimators. In fact, the charge range of a type II estimator with resistance calculated with (19) is presented with a formula based on a capacitance calculated with (16):

$$q_{range\text{-}II} = 2(C_S + C_P) A_S. \quad (21)$$

Section III findings can be summarised as following:

1. For type I/II charge estimators, (23)/(26) can theoretically calculate the sensing capacitance/ resistance leading to a sinusoidal voltage drop with an amplitude of A_S, where A_e is the amplitude of the sinusoidal excitation voltage.
2. Based on (16) and (19), the sensing capacitance/resistance of type I/II estimators is dependent on/independent of the excitation frequency. This is a merit for type I estimators.
3. A fixed component (bias) in excitation voltage leads to a fixed component voltage drop in type I estimators, as to (8) and superposition. Such a component (bias) has no enduring effect on the voltage drop in type II estimators, according to (15).
4. For an identical voltage drop, according to (17 and 21), type II estimators estimate larger charge compared to type I ones. However, the difference is insubstantial, considering (23) and assuming $A_e \gg 1$.

These analytical outcomes do not firmly support the superiority of type II resistor-based estimators, claimed in the literature. By the way, the presented analytical investigation is based on approximations and needs to be assessed and completed with experimentation.

IV. Experimentation

Figure 4 partly depicts the experimental setup, the implementation of Fig. 3. The same setup was used to implement Fig. 2 with change of the capacitor to a resistor. A personal computer with an Intel Core i7-2600 @ 3.4GHz CPU and a 12 GB RAM plays the role of the digital processor. Digital part of Figs.2 and 3 was implemented with use of MATLAB 9.1 /Simulink 8.8 software. Simulink Real-Time

Desktop Toolbox 5.3 was used to transfer the voltage signal to the computer through an A/D of a PCIe-6323 National Instruments multifunctional card. The actuator is a 7×7×42 mm^3 piezoelectric stack [27], with d_{31}= -270 pm/V, d_{33}=600 pm/V and the capacitance, C_P, of 6.23 µF, measured with an LCR metre at the amplitude of 1V and the frequency of 1 kHz and, V_e, the excitation voltage in Figs. 2 and 3, was originally generated in Simulink then transferred to an AETECHRON 7114 liner power amplifier through Simulink Real-Time Desktop Toolbox and the PCIe-6323 card.

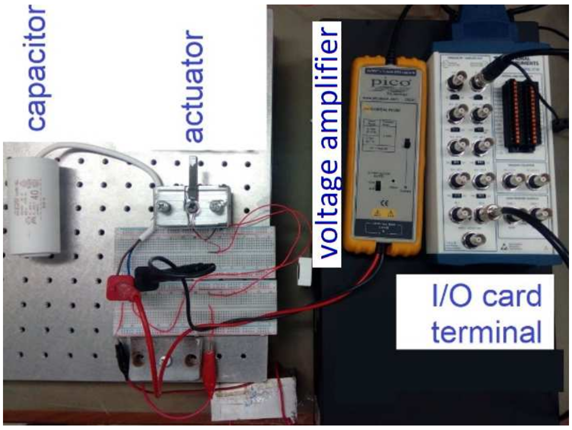

Fig. 4. Implementation of Fig 5, excluding the computer and the amplifier

As mentioned in sections II and III, the excitation voltages follows the equation of $V_e = A_e \sin \omega t$; excitation frequency in Hz is defined as $f_e = \omega/2\pi$. (22)

In order to have A_S=1 V, as mentioned in problem statement, with use of (9), in type I estimators, for the sensing capacitors of 20,40 and 80 µF, theoretical A_e would be 4.21, 7.42 and 13.84 V, respectively. A sinusoidal excitation voltage with each of these values of amplitude was applied on a setup with its respective sensing capacitor. Excitation frequency, f_e, has the values of 20,30,40,50,60 and 70 Hz for every single pair of capacitor and A_e. It means 18 experiments were performed to assess type I estimators. Similar experiments, with same values of A_e, were carried out for type II estimators; however, for each excitation frequency, the sensing resistance was calculated based on (19). In all experiments, range of charge, q_{range} and A_S (practically half of V_S range) were measured. The sample time of 10^{-4} s was used in all experiments.

V. Experimental Results and Discussion

With use of A_S=1 V, (16) and (19) lead to R_S and C_S, shown in (23) and (24).

$$C_S = C_P\left(A_e - 1\right) \ , \tag{23}$$

$$R_S = \frac{1}{C_P \omega \sqrt{A_e^2 - 1}}. \tag{24}$$

According to approximate analytical formulation presented in section III, sensing capacitance/resistance calculated with (23) and (24) should result in the sensing voltage amplitude (A_S) of 1 V and the range of charge as presented in (25) and (26) for any given sinusoidal excitation voltage with the amplitude of A_e. (25) and (26) are the results of A_S= 1 and (17) and (21). In summary, with R_S and C_S determined with (23) and (24), the following approximate theoretical outcomes are expected:

1. A_S=1 V
2. $q_{\text{range-}I} = 2C_S$. (25)
3. $q_{\text{range-}II} = 2(C_S + C_P)$. (26)

Tables I-III present the experimental results and their comparison with the aforementioned theoretical expectations of approximate analytical formulation, as shown in Fig.5. The following are three major observations out of these data:

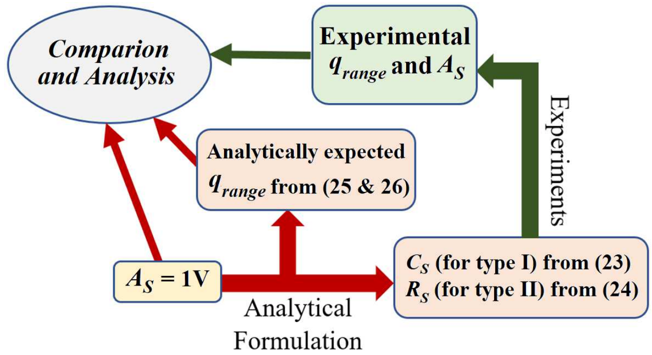

Fig. 5. Diagram of anlayis for a given A_e

A. Observation 1: difference of estimator types in frequency dependency

For each value of A_e, presented in Table I, II or III, voltage drop amplitude of type I estimators, $A_{S\text{-}I}$, and their range of charge, $q_{range\text{-}I}$, are nearly fixed across different excitation frequencies, f_e. This is in agreement with finding (ii) of analytical formulation of section III, presented in (9). On the other hand, in type II estimators, for higher values of A_e, presented in Tables II and III, $A_{S\text{-}II}$ and $q_{range\text{-}II}$ decrease meaningly with increase of f_e; although, the resistor changes with frequency according to (24) to maintain A_S at 1 V.

TABLE I. Experimental results for the excitation voltage amplitude of 4.21 V. Indice I and II refer to type I and II estiamtors.

	A_e=4.21 V , C_S=20 µF $q_{range\text{-}I\text{-}analytical}$=40 µC, $q_{range\text{-}II\text{-}analytical}$=52.46 µC				
f_e (Hz)	R (Ω)	$A_{S\text{-}I}$ (V)	$A_{S\text{-}II}$ (V)	$q_{range\text{-}I}$ (µC)	$q_{range\text{-}II}$ (µC)
20	303	1.10	0.99	44.14	53.07
30	202	1.10	1.00	44.08	54.62
40	152	1.10	1.00	44.01	54.35
50	121	1.10	1.02	43.88	54.19
60	101	1.10	0.97	43.94	52.77
70	87	1.10	0.96	43.94	53.64

TABLE II. Experimental results for the excitation voltage amplitude of 7.42 V. Indice I and II refer to type I and II estiamtors.

	A_e=7.42 V , C_S=40 µF $q_{range\text{-}I\text{-}analytical}$=80 µC, $q_{range\text{-}II\text{-}analytical}$=92.45 µC				
f_e (Hz)	R (Ω)	$A_{S\text{-}I}$ (V)	$A_{S\text{-}II}$ (V)	$q_{range\text{-}I}$ (µC)	$q_{range\text{-}II}$ (µC)
20	172	1.16	1.05	92.49	99.30
30	115	1.16	1.04	92.49	99.88
40	86	1.15	0.99	92.36	92.68
50	69	1.16	0.94	92.62	88.30
60	57	1.15	0.92	92.36	87.25
70	49	1.14	0.83	91.05	82.96

TABLE III. EXPERIMENTAL RESULTS FOR THE EXCITATION VOLTAGE AMPLITUDE OF 13.84 V. INDICE I AND II REFER TO TYPE I AND II ESTIAMTORS.

	A_e=13.84 V, C_S=80 µF $q_{range\text{-}I\text{-}analytical}$=160 µC, $q_{range\text{-}II\text{-}analytical}$=172 µC				
f_e (Hz)	R (Ω)	$A_{S\text{-}I}$ (V)	$A_{S\text{-}II}$ (V)	$q_{range\text{-}I}$ (µC)	$q_{range\text{-}II}$ (µC)
20	92	1.30	1.14	207.6	204.2
30	62	1.29	1.07	206.3	1 97.8
40	46	1.29	1.00	206.0	193.0
50	37	1.28	0.99	205.3	194.8
60	31	1.28	0.87	204.7	177.7
70	26	1.28	0.81	204.5	168.8

B. *Observation II: Discrepancy of theoretically expected and experimental values of A_S*

The real values of A_S, in most experiments, are not equal to 1V, despite theoretical expectations. This discrepancy simply means if (16) and (19) are trusted to find the capacitance/resistance of sensing components, an unexpected value of A_S may happen to exist. Particularly, too high values of A_S may lead to serious issues detailed in subsection VII.C of [20].

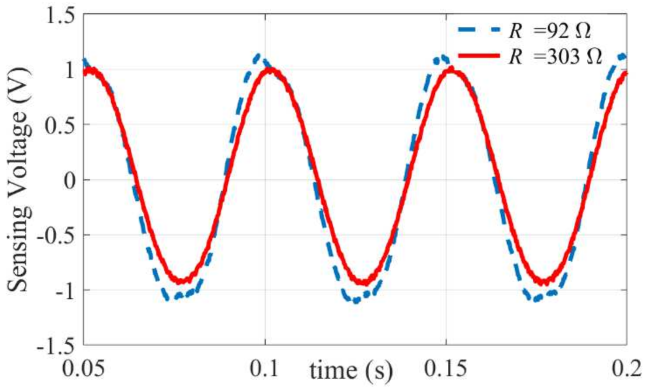

Fig. 6. The sesning voltage versus time for two type II estiamtors, with R=92 Ω and R=303 Ω excited with A_e=13.84 V and A_e=4.21 V, respectively, both with f_e=20 Hz, i.e the excitation voltages for each are 13.84sin(20×2πt) 4.21sin(20×2πt), repectively. Relevant cells in Tables I and III are sahded.

A partial reason of the difference between theoretical approximate expectations and the experimental results is neglected nonlinearities. As an instance, for type II estimators, based on the linearity of (19), it is expected that with a sinusoidal excitation voltage, V_e, a sinusoidal sensing voltage, V_S, is observed. Fig.6 depicts V_S of two type II estimators both designed with (24) and excited with sinusoidal voltage to assess this expectation. For the estimator designed for a higher amplitude of excitation voltage (A_e), V_S is not sinusoidal as shown by the dashed curve in Fig.6, relevant to the shaded cell in Table III; this demonstrates overlooked nonlinearity in analytical formulation. However, V_S of the other type II estimator, shown by a solid curve in Fig.6, relevant to the shaded cell of Table I, is nearly sinusoidal. This indicates that the nonlinearity is inapparent in some operating areas.

The mean value of the discrepancy between theoretically expected and experimental A_S, for type II estimators in Tables I, II and III are 0.0167 V, 0.0683 V and 0.09 V, respectively. These values are obviously larger for type I estimators, 0.1 V, 0.1533 V and 0.2867 V. However, the discrepancy can be avoided more simply in type I, as it is almost independent of frequency.

C. *Observation III: Type II estimators are capable of estimation of slightly higher values of charge*

The last observation is that Type II estimator can estimate higher values of charge compared to type I ones, with the same sensing voltage (voltage drop). This observation is in agreement with finding (iv) of analytical formulation in section IV, the outcome of comparison of (24) with (28) or (32) with (33).

The results presented in Tables I-III are not straightforwardly usable for this observation, as experimental values of A_S are different for type I and II estimators, particularly in Table III. Table IV, alternatively, eases the comparison. This table shows that, for the same amplitude of voltage drop (A_S), a type II estimator may estimate 12% to 40% higher amount of charge than a type I one, for the setup and conditions detailed in section V. However, this discrepancy is not as substantial as presented in experimental results reported in [21]. As an instance, for the excitation frequency of 10 Hz, the result of Table 2 of [21] can be reasonably interpreted as type II estimators can estimate 892% more charge than type I ones with the same A_S. Such results have been used as a ground for superiority of type II estimators. The point is that [21] lacks a deep enough analytical formulation and its consequent design method; hence, the experiments were practically carried out with intuitively chosen values of R_S and C_S.

VI. CONCLUSION

This paper compares the most recent/effective types of charge estimators for piezoelectric actuators: the estimators with a sensing capacitor, named type I, and the estimators with a sensing resistor, named type II in the paper. The latter is also known as digital estimator. In order to have an even-handed comparison, the digital version of type I estimator, depicted in Fig.3, was developed and implemented.

TABLE IV. EXPERIMTAL RESULTS FOR THREE AMPLITUDES OF EXCITATION VOLTAGE. INDICE I AND II REFER TO TYPE I AND II ESTIAMTORS.

	A_e=4.21 V C_S=20 µF		A_e=7.42 V C_S=40 µF		A_e=13.84 V C_S=80 µF	
f_e (Hz)	$\frac{q_{range\text{-}I}}{A_{S\text{-}I}}$	$\frac{q_{range\text{-}II}}{A_{S\text{-}II}}$	$\frac{q_{range\text{-}I}}{A_{S\text{-}I}}$	$\frac{q_{range\text{-}II}}{A_{S\text{-}II}}$	$\frac{q_{range\text{-}I}}{A_{S\text{-}I}}$	$\frac{q_{range\text{-}II}}{A_{S\text{-}II}}$
20	40	53.60	80	94.20	160	179.4
30	40	54.53	80	96.40	160	185.3
40	40	54.53	80	93.77	160	193.0
50	40	53.23	80	93.87	160	196.1
60	40	54.20	80	94.40	160	203.5
70	40	56.04	80	99.69	160	209.1

In both type I and II estimators, a portion of the excitation voltage is squandered for charge estimation and does not apply on the actuator; this wasted voltage is called voltage drop. Comparative experimental results in the literature demonstrate that, with the same voltage drop, type II estimators can estimate significantly higher charge than type I ones, in similar operating conditions. As a result, type II estimators were widely considered superior in the last decade. This paper reports a through analytical and experimental comparative study to assess the claimed superiority of type II estimators in terms of voltage drop and other aspects. The following are the main conclusions of this study:

C1. Type II estimators have slightly higher ratio of estimated charge to voltage drop, 12% to 40% according to experiments.

C2. Both behaviour and the choice of the sensing element are independent of/dependent on frequency in type I/II estimators, as a major advantage of type I ones.

C3. Bias (time-independent component) of the excitation voltage has an/no enduring effect on the behaviour of type I/II estimators.

C4. In type I estimators, in order to have low voltage drops, high capacitance sensing capacitors need to be employed. These capacitors are bulkier than the resistors used in type II estimators. Such a capacitor is shown in Fig.4.

C5. Type I estimators can be implemented as an analogue circuit, e.g. Fig.1; while, type II ones need digital processors to be implemented.

In summary, both type I and II may be usable for different applications based on priorities of the design, and none can be put aside.

References

[1] I. Chopra, "Review of state of art of smart structures and integrated systems," *Aiaa Journal,* vol. 40, no. 11, pp. 2145-2187, Nov 2002.

[2] S. Rios and A. Fleming, "Control of Piezoelectric Benders Using a Charge Drive," in *14th International Conference on New Actuators,*, Beremen, Germany, 2014, 2014.

[3] S. O. R. Moheimani, "Invited Review Article: Accurate and fast nanopositioning with piezoelectric tube scanners: Emerging trends and future challenges," *Review of Scientific Instruments,* vol. 79, no. 7, p. 071101, Jul 2008.

[4] M. Mohammadzaheri and A. AlQallaf, "Nanopositioning systems with piezoelectric actuators, current state and future perspective," *Science of Advanced Materials,* vol. 9, no. 7, pp. 1071-1080, 2017.

[5] C. Hu, Y. Shi, and F. Liu, "Research on Precision Blanking Process Design of Micro Gear Based on Piezoelectric Actuator," *Micromachines,* vol. 12, no. 2, pp. 200-209, 2021.

[6] J. Deng, S. Liu, Y. Liu, L. Wang, X. Gao, and K. Li, "A 2-DOF Needle Insertion Device Using Inertial Piezoelectric Actuator," *IEEE Transactions on Industrial Electronics,* vol. 69, no. 4, pp. 3918-3927, 2021.

[7] M. Mohammadzaheri, P. Soltani, and M. Ghodsi, "Micro/Nanopositioning Systems with Piezoelectric Actuators and Their Role in Sustainability and Ecosystems," in *EcoMechatronics*: Springer, 2022, pp. 233-250.

[8] W. K. Szeremeta, R. L. Harniman, C. R. Bermingham, and M. Antognozzi, "Towards a Fully Automated Scanning Probe Microscope for Biomedical Applications," *Sensors,* vol. 21, no. 9, pp. 3027-3040, 2021.

[9] W. Meinhold, D. E. Martinez, J. Oshinski, A.-P. Hu, and J. Ueda, "A direct drive parallel plane piezoelectric needle positioning robot for MRI guided intraspinal injection," *IEEE Transactions on Biomedical Engineering,* vol. 68, no. 3, pp. 807-814, 2020.

[10] N. Miri, M. Mohammadzaheri, and L. Chen, "An enhanced physics-based model to estimate the displacement of piezoelectric actuators," *Journal of Intelligent Material Systems and Structures,* vol. 26, no. 11, pp. 1442-1451, 2015.

[11] M. Bazghaleh, S. Grainger, M. Mohammadzaheri, B. Cazzolato, and T.-F. Lu, "A novel digital charge-based displacement estimator for sensorless control of a grounded-load piezoelectric tube actuator," *Sensors and Actuators A: Physical,* vol. 198, pp. 91-98, 2013.

[12] D. Soleymanzadeh, H. Ghafarirad, and M. Zareinejad, "Charge-based robust position estimation for low impedance piezoelectric actuators," *Measurement,* vol. 147, p. 106839, 2019.

[13] M. Mohammadzaheri; *et al.*, "Adaptive Charge Estimation of Piezoelectric Actuators, a Radial Basis Function Approach," presented at the 20th International Conference on Research and Education in Mechatronics Wels, Austria 23-24 May, 2019.

[14] M. Mohammadzaheri, S. AlSulti, M. Ghodsi, I. Bahadur, and M. Emadi, "Assessment of capacitor-based charge estimators for piezoelectric actuators," in *IEEE International Conference on Mechatronics*, 2021, pp. 1-6: IEEE.

[15] M. Bazghaleh, S. Grainger, M. J. J. o. I. M. S. Mohammadzaheri, and Structures, "A review of charge methods for driving piezoelectric actuators," *Journal of Intelligent Material Systems and Structures,* vol. 29, no. 10, pp. 2096-2104, 2018.

[16] R. H. Comstock, "Charge control of piezoelectric actuators to reduce hysteresis effects," ed: Google Patents, 1981.

[17] M. Bazghaleh, S. Grainger, B. Cazzolato, and T.-f. Lu, "An innovative digital charge amplifier to reduce hysteresis in piezoelectric actuators," presented at the Australian Robotics and Automation Association (ACRA), Brisbane, Australia, December, 2010.

[18] M. Mohammadzaheri, H. Ziaiefar, and M. Ghodsi, "Digital Charge Estimation for Piezoelectric Actuators: An Artificial Intelligence Approach," in *Handbook of Research on New Investigations in Artificial Life, AI, and Machine Learning*: IGI Global, 2022, pp. 117-140.

[19] M. Bazghaleh, S. Grainger, B. Cazzolato, and T. Lu, "Using frequency-weighted data fusion to improve the performance of a digital charge amplifier," in *IEEE International Conference on Robotics and Automation*, Saint Paul, USA, 2012, pp. 4774-4779: IEEE.

[20] M. Mohammadzaheri *et al.*, "Adaptive Charge Estimation of Piezoelectric Actuators with a Variable Sensing Resistor, an Artificial Intelligence Approach," *Engineering Letters,* vol. 30, no. 1, pp. 193-200, 2022.

[21] M. Bazghaleh, S. Grainger, M. Mohammadzaheri, B. Cazzolato, and T. Lu, "A digital charge amplifier for hysteresis elimination in piezoelectric actuators," *Smart Materials and Structures,* vol. 22, no. 7, p. 075016, 2013.

[22] J. Zhong, R. Nishida, and T. Shinshi, "A digital charge control strategy for reducing the hysteresis in piezoelectric actuators: Analysis, design, and implementation," *Precision Engineering,* vol. 67, pp. 370-382, 2021.

[23] A. J. Fleming and R. Moheimani, "Improved current and charge amplifiers for driving piezoelectric loads, and issues in signal processing design for synthesis of shunt damping circuits," *Journal of Intelligent Material Systems and Structures* vol. 15, no. 2, pp. 77-92, 2004.

[24] A. J. Fleming and S. O. R. Moheimani, "A grounded-load charge amplifier for reducing hysteresis in piezoelectric tube scanners," *Review of Scientific Instruments,* vol. 76, no. 7, pp. 0737071-5, 2005.

[25] M. Bazghaleh, M. Mohammadzaheri, S. Grainger, B. Cazzolato, and T. F. Lu, "A new hybrid method for sensorless control of piezoelectric actuators," *Sensors and Actuators A: Physical,* vol. 194, pp. 25-30, 2013.

[26] M. Mohammadzaheri, M. Emadi, M. Ghodsi, I. M. Bahadur, M. Zarog, and A. Saleem, "Development of a Charge Estimator for Piezoelectric Actuators: A Radial Basis Function Approach," *International Journal of Artificial Intelligence and Machine Learning,* vol. 10, no. 1, pp. 31-44, 2020.

[27] PiezoDrive. (2023). *Piezoelectric Actuators*. Available: https://www.piezodrive.com/actuators/150v-piezo-stack-actuators-2/